Comparison of Electron-Atom Collision Parameters for S to P Transitions under Reversal of Energy Transfer

M. Shurgalin,[1,*] A. J. Murray,[1] W. R. MacGillivray,[1,†] M. C. Standage,[1] D. H. Madison,[2] K. D. Winkler,[2] and I. Bray[3]
[1]*Laser Atomic Physics Laboratory, School of Science, Griffith University, Brisbane, Queensland, 4111, Australia*
[2]*Laboratory for Atomic, Molecular and Optical Research, University of Missouri-Rolla, Rolla, Missouri 65401*
[3]*Electronic Structure of Materials Centre, Flinders University, Adelaide, South Australia 5001, Australia*
(Received 1 May 1998)

Inelastic and superelastic electron scattering from the optically prepared $3^2P_{3/2}$ state of sodium has enabled atomic collision parameters to be deduced for the $4S$-$3P$ deexcitation and the $3S$-$3P$ excitation processes. These data are compared with convergent close coupling and second order distorted wave Born calculations. For excitation, both theories agree with experiment, whereas for deexcitation the close coupling theory is in better agreement. A long-standing proposal relating to the sign of the transferred angular momentum is not supported. [S0031-9007(98)07775-8]

PACS numbers: 34.80.Dp

Extensive studies of electron collision-induced atomic transitions involving the ground state performed over the last 25 years have resulted in a substantial body of experimental data and have stimulated the development of a number of theoretical models ([1–3], and references therein). By contrast, few investigations have been devoted to electron-impact excitation of transitions between *excited* atomic states [4–7]. Theoretical models of electron-impact excitation, developed for atoms initially in the strongly bound ground state, may not be applicable for transitions between excited states that are less strongly bound to the atomic core. Electron excitation involving excited states plays an important role in electrical discharges, astrophysics, and in many branches of plasma physics, and so the study of these processes is of relevance in a number of different fields.

Experimental techniques, such as electron-photon coincidence and superelastic methods, allow measurements of comprehensive sets of observables called the atomic collision parameters (ACPs), which directly relate to the complex scattering amplitudes. ACP measurements complement excitation differential cross section (DCS) measurements while providing more sensitive tests of different theoretical models. When the spin of the incident and scattered electron is not measured, a subset of the complete set of collision parameters is obtained. For transitions between S and P states for which spin-orbit interactions are negligible, four spin unresolved ACPs are required: the angular momentum transferred perpendicular to the scattering plane $L_\perp$, the degree of anisotropy of the atomic charge cloud P_ℓ, the charge cloud alignment angle γ, and the degree of coherence P^+ [3].

Of particular interest is the behavior of $L_\perp$ as a function of scattering angle [8–10]. An analysis of general trends in the behavior of this parameter was performed in 1981 by Madison and Winters [11]. By expressing this parameter in terms of a Born series expansion for the transition matrix up to second order, their analysis indicated that for a ground S state to excited P state transition, $L_\perp$ should be positive at small scattering angles and negative at larger angles. This qualitative prediction was supported for sodium by calculations using a second order distorted wave Born (DWB2) theory [12] and by experiment [13].

Madison and Winters further proposed that for a positive projectile (i.e., for positron scattering), $L_\perp$ would be negative at all scattering angles. Based on this Born series expansion, Andersen and Hertel [14] suggested that a reversal of energy transfer for electron scattering should have a similar effect on the $L_\perp$ parameter. Consequently, $L_\perp$ should be negative at all scattering angles for electron impact deexcitation from an S to a P state. One of the principal aims of the experimental investigations presented here was to test these assertions while additionally providing a set of ACPs for the excited state transition.

Two main techniques are currently used to obtain ACPs for transitions involving the ground state. In electron-photon coincidence experiments, inelastically scattered electrons are detected in coincidence with fluorescence photons emanating from the decay of the excited atoms. Polarization analysis of the fluorescence enables the ACPs to be deduced. Alternatively, superelastic scattering experiments prepare the target atoms in a known excited state with coherent laser radiation. The superelastically scattered electron rate is then measured as a function of laser polarization and scattering angle. This allows the ACPs to be obtained since the deexcitation process can be regarded as the time inverse of the excitation process [3].

A technique similar to superelastic scattering is used here to measure ACPs for transitions between *excited* atomic P and S states. The difference is that the *inelastically* scattered electrons inducing P to S state transitions are detected. These experiments, performed in the "time-inverse" geometry, allow information to be obtained about the electron-impact deexcitation from an S to a P state. A theory detailing these measurements which exploits the principle of microreversibility has been presented [15].

The first excited state ACP measurements for sodium were performed by Hermann *et al.* [6]. However, only

 0031-9007/98/81(21)/4604(4)$15.00

two parameters were measured over a limited range of scattering angles from 5° to 10°. No measurements of the $L_\perp$ parameter were reported. No experimental results reported so far have allowed a test of the behavior of the $L_\perp$ parameter when the energy transfer between the incident electron and target atom is reversed.

In this Letter, the first measurements of ACPs for the electron-impact induced $4S$-$3P$ transition in sodium are reported. The measurements are compared with convergent close coupled (CCC) and DWB2 calculations. Sodium provides an excellent candidate for a study of the scattering process between excited states since the $4S$ state of sodium is energetically more than halfway between the ground state and the ionization threshold. The electron is therefore more weakly bound to the atomic core, and this may play a role in the interaction process. The $4S$ state is the next excited state above the $3P$ state and is well separated from all other states.

Investigation of the $3S$ to $3P$ and $4S$ to $3P$ transitions in sodium allows the differences between electron-impact excitation and deexcitation to be investigated, providing an ideal test bed for the proposals discussed above. In both the $3S$ to $3P$ and $4S$ to $3P$ transitions, angular momentum is transferred from the projectile electron to the target atom, but in the former case the atom *gains* energy while in the latter case energy is lost. The $3S$ to $3P$ transition has been extensively investigated [16]. However, to allow direct comparison not influenced by differences in experimental conditions, measurements for the $3S$ to $3P$ transition were performed simultaneously with $4S$ to $3P$ measurements in the same apparatus during this work.

Experimentally, the ACPs were determined from the pseudo-Stokes parameters obtained by measuring the scattered electron count rate from the laser excited state as a function of laser polarization in the time-inverse geometry [15]. Laser radiation, tuned to excite the $3P_{3/2}$ state of sodium is propagated perpendicular to the scattering plane defined by the incident electron beam and the scattered electron directions. The pseudo-Stokes parameters are given by [17]

$$P_1^S(\theta) = \frac{S_0(\theta) - S_{90}(\theta)}{S_0(\theta) + S_{90}(\theta)},$$
$$P_2^S(\theta) = \frac{S_{45}(\theta) - S_{135}(\theta)}{S_{45}(\theta) + S_{135}(\theta)}, \qquad (1)$$
$$P_3^S(\theta) = \frac{S_{\mathrm{RHC}}(\theta) - S_{\mathrm{LHC}}(\theta)}{S_{\mathrm{RHC}}(\theta) + S_{\mathrm{LHC}}(\theta)},$$

where $S_\phi(\theta)$ is the scattered electron count rate from the target excited with linearly polarized laser light with polarization angle φ to the direction of the scattered electron θ, and $S_{\mathrm{RHC}}(\theta)$ and $S_{\mathrm{LHC}}(\theta)$ are the scattered electron count rates from atoms excited with right-hand and left-hand circularly polarized laser light, respectively. A description of the experimental apparatus is given in [15]. The ACPs are deduced according to the formulas [3]

$$L_\perp = -\frac{P_3^S}{K'}, \qquad P_1 = \frac{1}{K}\sqrt{(P_1^S)^2 + (P_2^S)^2},$$
$$\gamma = \frac{1}{2}\tan^{-1}\left(\frac{P_2^S}{P_1^S}\right) \pm \frac{\pi}{2}, \qquad P^+ = \sqrt{P_1^2 + L_\perp^2}, \qquad (2)$$

where K and K' are optical pumping parameters accounting for hyperfine interactions during laser excitation with linear and circular polarizations, respectively.

The optical pumping parameters were calculated using a full QED description of the laser excitation process [17] and were found to be $K = 0.36$ and $K' = -0.99$ for the experimental conditions used in this work. The K parameter, which is sensitive to laser frequency tuning and intensity, was also verified experimentally from the fluorescence line polarization.

The pseudo-Stokes parameters were measured for the $3P$-$3S$ and $3P$-$4S$ transitions at incident electron energies of 19.9 and 23.1 eV, respectively, corresponding to an equivalent incident electron energy of 22 eV for the excitation and deexcitation processes. Figures 1–4 show the ACPs as functions of scattering angle for (a) the $4S$-$3P$ transition and (b) the $3S$-$3P$ transition. The experimental uncertainties shown are 1 standard deviation. These figures also show the results of the DWB2 and CCC calculations.

The behavior of the $L_\perp$ parameter for $4S$-$3P$ deexcitation is found to be very different from $L_\perp$ for $3S$-$3P$ excitation (Fig. 1). For the $3S$-$3P$ transition, $L_\perp$ is positive for positive scattering angles and increases with scattering

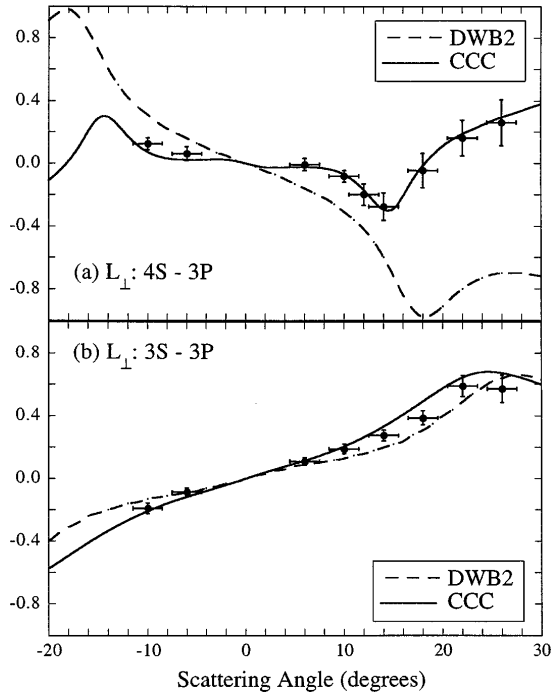

FIG. 1. The $L_\perp$ parameter for (a) the $4S$-$3P$ and (b) the $3S$-$3P$ transitions as a function of scattering angle. The solid lines show the CCC calculations, whereas the dashed lines show the DWB2 calculations.

angle reaching a maximum of approximately 0.7 at a scattering angle around 24°. This behavior is in accord with the qualitative predictions discussed above. Both the CCC and DWB2 calculations are in agreement with measurements.

From the $4S$-$3P$ transition, the situation is quite different. For this transition, $L_\perp$ is almost zero at scattering angles below 8°, then decreases to a negative value of -0.25 at a scattering angle of 15° in accordance with the suggestion of Andersen and Hertel [14] that $L_\perp$ should be negative for the $4S$-$3P$ transition. However, at higher scattering angles $L_\perp$ inverts and becomes positive, increasing to larger values with increasing scattering angle. This behavior is not predicted by the qualitative arguments presented above. The CCC calculation is in excellent agreement with experiment, whereas the DWB2 calculation predicts values much greater than determined experimentally, reaching almost unity (full orientation) at $\pm 20°$. It is curious that the DWB2 is in better agreement with the data for $3S$-$3P$ than $4S$-$3P$. Since the energy transfer for $4S$-$3P$ is smaller than $3S$-$3P$, one would expect a perturbative approach to be better for the $4S$-$3P$ transition. An examination of the contribution of first and second order effects in distorted wave calculations reveals that, out to scattering angles of 20°, $L_\perp$ is dominated by first order effects. The Born approximation, on the other hand, predicts zero for $L_\perp$ which is arguably closer to the $4S$-$3P$ data than the distorted wave results. Consequently, first order distortion is producing unphysically large results for $L_\perp$ for the excited state.

The P_l parameter (Fig. 2) is similar for the $3S$-$3P$ and $4S$-$3P$ transitions for small scattering angles which at approximately 0.85 indicates a high degree of charge cloud anisotropy. Within experimental uncertainty, P_l then decreases for scattering angles greater than 15° for both transitions. Both the CCC and DWB2 calculations predict P_l reasonably well for the $3S$-$3P$ transition. However, for the $4S$-$3P$ transition the CCC calculation predicts noticeably larger values than experiment, whereas the DWB2 calculation appears in better agreement. This agreement may be fortuitous, since the large value of the $L_\perp$ parameter at $\pm 20°$ predicted by the DWB2 calculation requires that the P_l parameter must reduce to close to zero at these angles since $P_l^2 + L_\perp^2 \leq 1$.

In the first Born approximation, the alignment angle γ is the angle between the beam direction and the momentum transfer direction [3,18]. In this approximation, γ will be negative for $3S$-$3P$ and positive for $4S$-$3P$. Typically, experimental and theoretical results for γ are close to the Born approximation, and it has been pointed out that the orientation of the charge cloud relative to the momentum transfer direction is more interesting than the deviation from the beam direction [18]. Experimental and theoretical results for γ are presented in Fig. 3. The two cases follow the prediction of the Born approximation with γ being negative for $3S$-$3P$ and positive for $4S$-$3P$. In fact, the good agreement between the data and the Born

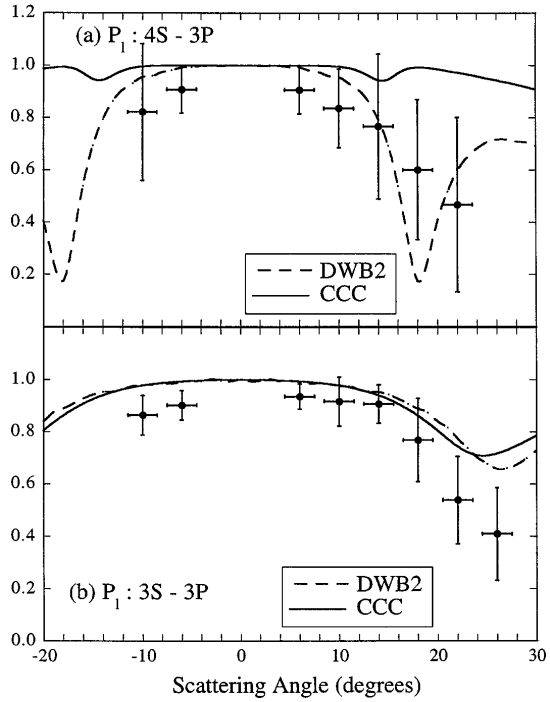

FIG. 2. The P_l parameter for (a) the $4S$-$3P$ and (b) the $3S$-$3P$ transitions as a function of scattering angle. Circles present the current experimental measurements. The solid lines show the CCC calculations, whereas the dashed lines show the DWB2 calculations.

results demonstrates that the charge cloud is nearly aligned with the momentum transfer direction in this angular range. Both the DWB2 and CCC are in close accord with each other and the experiment for the $3S$-$3P$ transition. For the $4S$-$3P$ transition, the CCC calculation provides very close agreement to the experimental data, while the DWB2 model agrees within 1 standard deviation at all but one data point. The structure in the DWB2 near 20° results from a minimum in P_1 occurring at the same angle that P_2 passes through zero which means that it is quite sensitive to the details of the calculation.

The P^+ parameter (Fig. 4) provides information about the significance of spin exchange in electron-atom collisions. In the absence of spin exchange P^+ is unity [1–3]. For the $3S$-$3P$ excitation, P^+ is found to be near unity at small scattering angles, decreasing slightly at 18° to 26° thereby indicating (within 1 standard deviation) some spin-exchange effects. A small spin-exchange effect is predicted by the DWB2 calculation for this transition, in contrast to the CCC model. For the $4S$-$3P$ deexcitation, both theories predict the P^+ parameter to be very close to unity. By contrast, within 1 standard deviation, the experimental results for the $4S$-$3P$ transition yield values of P^+ below unity at angles of 18° and 22°. This may indicate some spin-exchange effects at these scattering angles although the error bars are large at these angles.

The set of ACPs for the $4S$-$3P$ transition presented here clearly differ from those for the $3S$-$3P$ transition

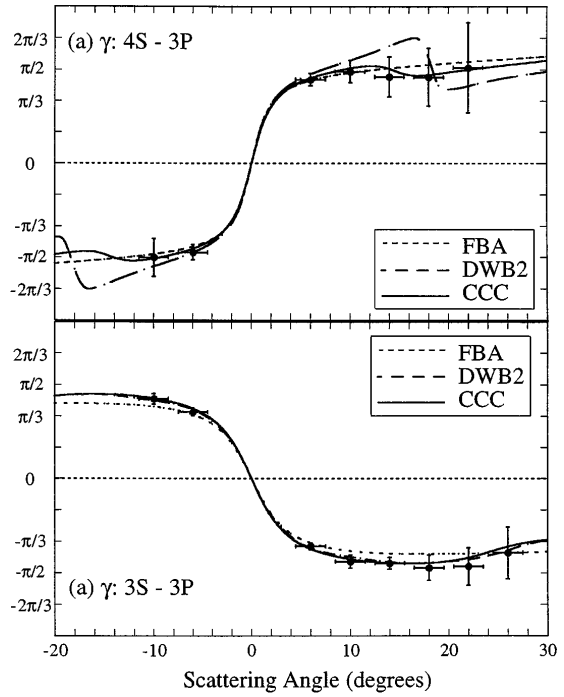

FIG. 3. The γ parameter for (a) the $4S$-$3P$ and (b) the $3S$-$3P$ transitions as a function of scattering angle. The solid lines show the CCC calculations, the full dashed lines show the DWB2 calculations, and the smaller dashed lines are the first Born results.

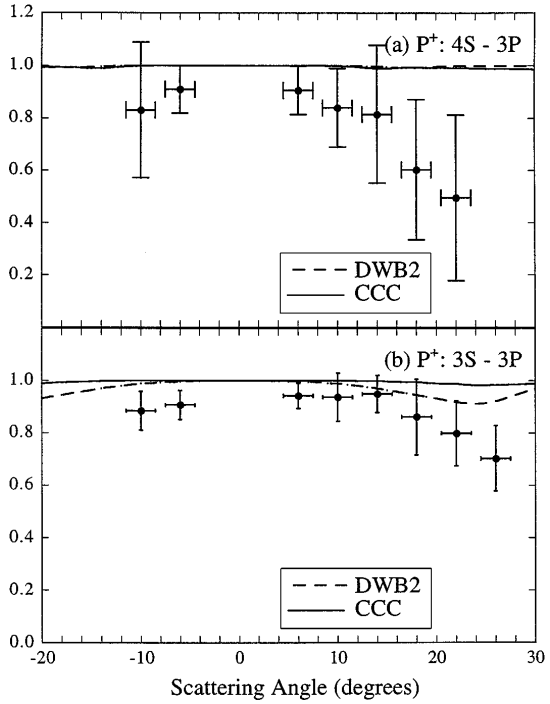

FIG. 4. The P^+ parameter for (a) the $4S$-$3P$ and (b) the $3S$-$3P$ transitions as a function of scattering angle. The solid lines show the CCC calculations, whereas the dashed lines show the DWB2 calculations.

and contain more angular structure. The suggestion of Andersen and Hertel [14] that the $L_\perp$ parameter for the $4S$-$3P$ transition should have a different sign from the $3S$-$3P$ transition is supported only for scattering angles below 10° to 12°.

The CCC and DWB2 models, which are both successful for the $3S$-$3P$ transition, are in less accord with each other and with the measurements for the $4S$-$3P$ transition. The CCC is in excellent agreement with experiments for $L_\perp$ and γ. For P_l and P^+, on the other hand, the CCC predicts values near unity while the experimental results suggest significant nonunity values. The DWB2 predicts nearly unity for P^+ and a significant deviation for P_l in agreement with experiment. This agreement may be fortuitous, however, since the DWB2 is significantly larger than the experiment for $L_\perp$. The experimental results for the P^+ parameter indicate more significant spin-exchange effects for the $4S$-$3P$ transition than for the $3S$-$3P$ transition as well as more significant spin-exchange effects than either theory predicts. However, the experimental error bars are large so further experiments with reduced uncertainty and at larger scattering angles are clearly desirable. If improved measurements support the present findings, further theoretical investigations of the importance of spin exchange will be warranted.

This work has been supported by the Australian Research Council and the U.S. Natural Science Foundation. The authors acknowledge helpful discussions with K. Bartschat.

*Present address: Harvard-Smithsonian Centre for Astrophysics, Cambridge, MA 02138.
†To whom correspondence should be addressed.
Electronic address: W.MacGillivray@sct.gu.edu.au

[1] N. Andersen *et al.*, Phys. Rep. **279**, 251 (1997).
[2] N. Andersen and K. Bartschat, Adv. At. Mol. Opt. Phys. **36**, 1 (1996).
[3] N. Andersen *et al.*, Phys. Rep. **165**, 1 (1988).
[4] C. C. Lin and L. W. Anderson, Adv. At. Mol. Opt. Phys. **29**, 1 (1992).
[5] S. Trajmar and J. C. Nickel, Adv. At. Mol. Opt. Phys. **30**, 45 (1993).
[6] H. W. Hermann *et al.*, J. Phys. B **10**, 251 (1977).
[7] G. A. Peach *et al.*, Phys. Rev. Lett. **81**, 309 (1998).
[8] H. W. Hermann *et al.*, J. Phys. B **13**, 3465 (1980).
[9] N. Andersen *et al.*, J. Phys. B **17**, L901 (1984).
[10] D. H. Madison *et al.*, J. Phys. B **19**, 3361 (1986).
[11] D. H. Madison and K. H. Winters, Phys. Rev. Lett. **47**, 1885 (1981).
[12] V. E. Bubelev *et al.*, J. Phys. B **29**, 1751 (1996).
[13] R. E. Scholten *et al.*, J. Phys. B **24**, L653 (1991).
[14] N. Andersen and I. Hertel, Comments At. Mol. Phys. **19**, 1 (1986).
[15] M. Shurgalin *et al.*, J. Phys. B **31**, 4205 (1998).
[16] See, for example, [3], and references therein; R. E. Scholten *et al.*, J. Phys. B **26**, 987 (1993); R. T. Sang *et al.*, J. Phys. B **27**, 1187 (1994).
[17] P. M. Farrell *et al.*, Phys. Rev. A **44**, 1828 (1991).
[18] N. Andersen and K. Bartschat, J. Phys. B **30**, 5071 (1997).